

Falkenburger et al., <http://www.jgp.org/cgi/content/full/jgp.201210887/DC1>

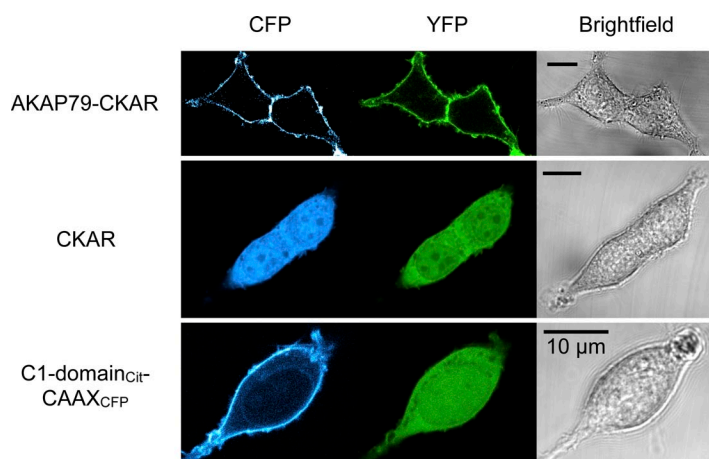


Figure S1. Expression patterns of FRET probes. Cells were transfected with the indicated plasmids and imaged by confocal microscopy (63× objective; 710 microscope; Carl Zeiss). The 405- and 516-nm laser lines were used for excitation of CFP and YFP. Emission was collected from 460 to 480 nm and from 540 to 560 nm. Note plasma membrane localization of AKAP-CKAR and CFP-CAAX and the cytosolic localization of CKAR and C1-YFP in resting cells.

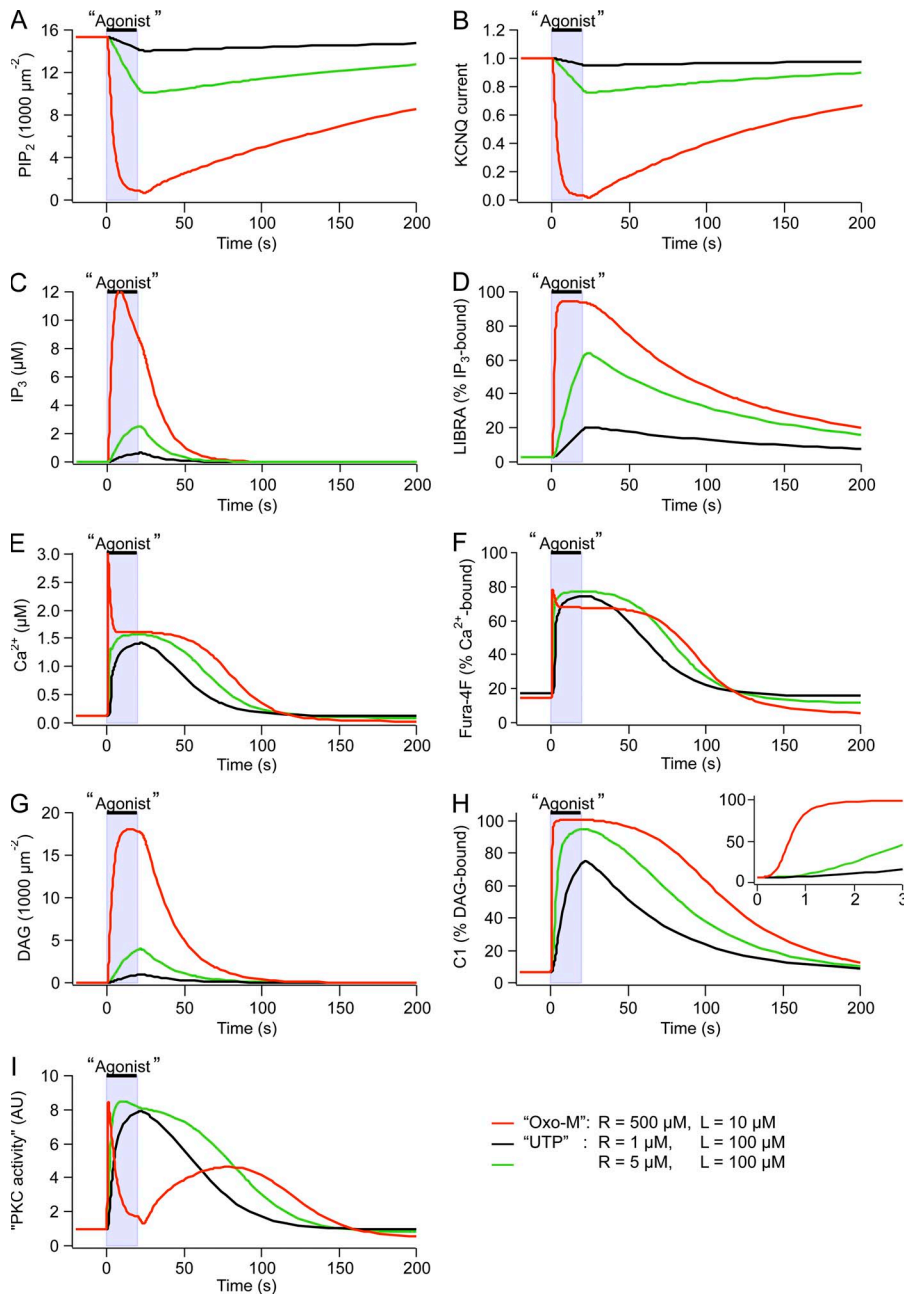


Figure S2. Model predictions comparing Oxo-M with UTP by assuming a simple variation of receptor density with no change of receptor properties. (A–I) Lines represent time courses predicted for the indicated species, density of receptors (“R”), and agonist concentrations (“L”). A receptor density of $500 \mu\text{m}^{-2}$ is our representation of high-density expressed M_1 Rs; a receptor density of $5 \mu\text{m}^{-2}$ is the density estimated for eP2Y₂Rs from Western blot analysis (Dickson et al. 2013. *J. Gen. Physiol.* <http://dx.doi.org/10.1085/jgp.201210886>); a density of $1 \mu\text{m}^{-2}$ best reproduces our experimental findings for eP2Y₂Rs and corresponds to the density of endogenous receptors expected from typical ratios of receptors to G proteins (Falkenburger et al. 2010. *J. Gen. Physiol.* 135:81–97). The calculation assumes that the “receptor K_d ” for UTP is the same as that for Oxo-M. In fact, K_{UTP} may be a little higher than K_{Oxo-M} . (I) An approximate prediction of PKC activity computed essentially as follows: $\text{DAG} * \text{PIP}_2 / ((\text{DAG} + K_{DC1}) * (\text{PIP}_2 + K_{DPH}))$, where K_{DC1} is the dissociation constant of the complex DAG–C1 domain (from PKC), and K_{DPH} is the dissociation constant of the complex PIP_2 –PH domain for PIP_2 (as a proxy for the unknown affinity of the PKC C2 domain for PIP_2). [LIBRAvIII] was $6 \mu\text{M}$ for D and 0 for all other panels. [Fura-4F] was $1 \mu\text{M}$ for F and 0 for all other panels. [C1] was $0.5 \mu\text{M}$ for H and 0 for all other panels.

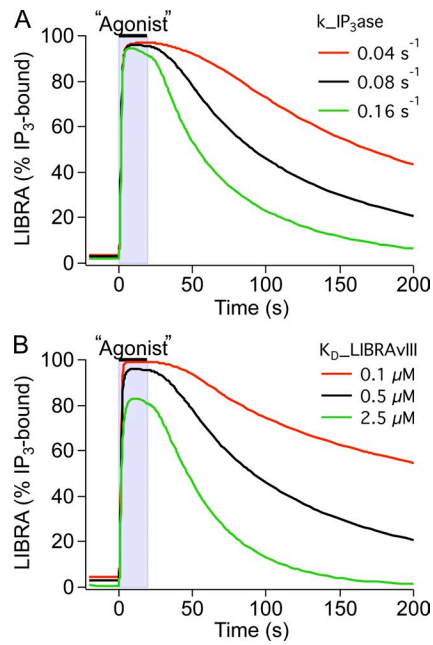


Figure S3. Dependence of the LIBRAvIII response on parameters k_{IP_3ase} and $K_D_{LIBRAvIII}$. Computed time courses from the model for the percentage of IP₃-bound LIBRAvIII, demonstrating the effects of changing the rate constant for IP₃ clearance (k_{IP_3ase} ; A) or the dissociation constant of LIBRAvIII ($K_D_{LIBRAvIII}$; B). [LIBRAvIII] was 6 μM. The final model parameters used in other figures (see Table 2 in main text) correspond to the middle value (black traces) in each panel of this figure.

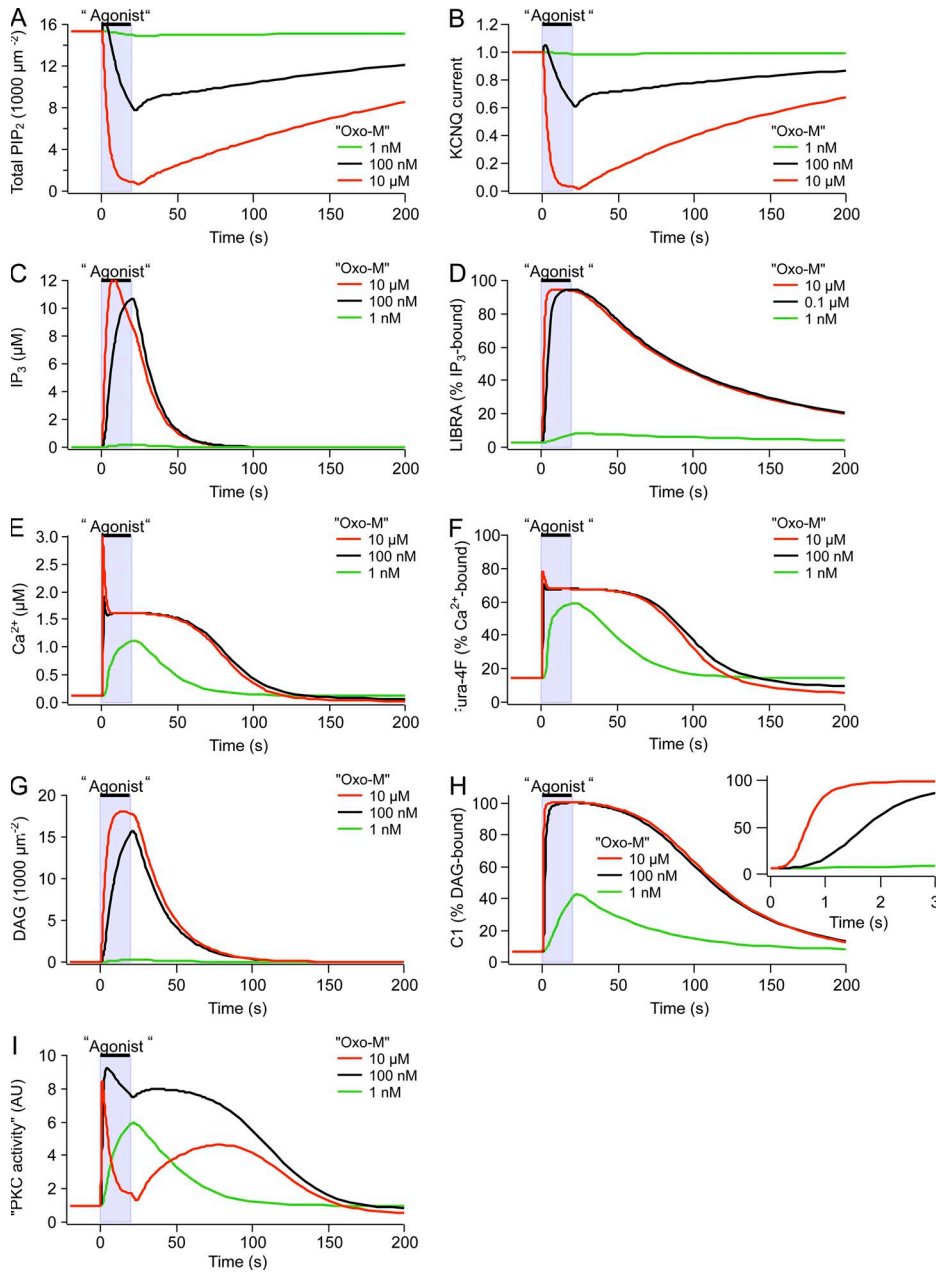


Figure S4. Model predictions for a concentration series of Oxo-M. (A–I) Simulated time courses from the model for the indicated species and Oxo-M concentrations. The inset in H shows an enlarged x axis to better appreciate the delayed onset with 100 nM as compared with 10 μ M Oxo-M. (I) An approximate prediction of PKC activity computed as in Fig. S2 I. [LIBRAvIII] was 6 μ M for D and 0 for all other panels. [Fura-4F] was 1 μ M for F and 0 for all other panels. [C1] was 0.5 μ M for H and 0 for all other panels.

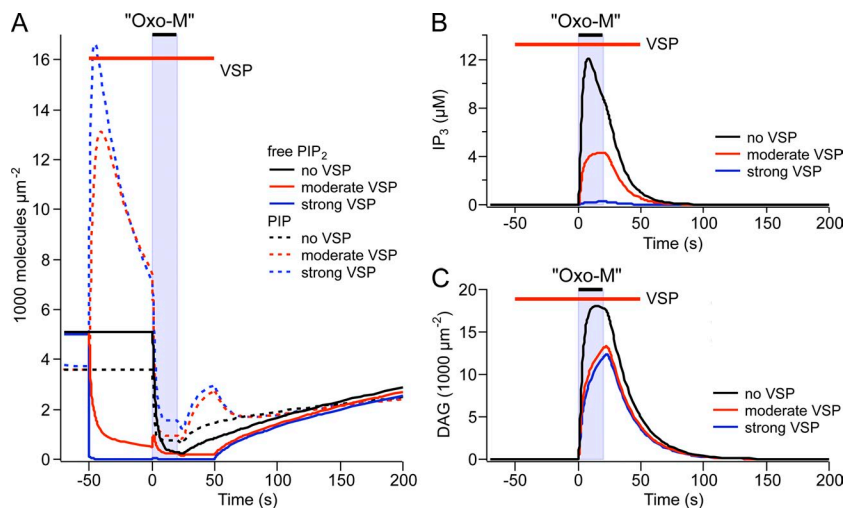


Figure S5. Computational study of VSP activation during Oxo-M. (A) Computed time courses of PI(4)P (PIP) and PIP_2 in the same simulation as in Fig. 4 (G and H) in the main text. Note the increase in PI(4)P resulting from VSP activation and its relaxation to rest partly through the PI 4-phosphatase. (B) Computed time course of IP_3 in a simulation as in Fig. 4 (G and H) in the main text, except that $[\text{LIBRAvIII}]$ was $0 \mu\text{M}$. (C) Computed time course of DAG in a simulation as in Fig. 4 (G and H) in the main text, except that $[\text{C1}]$ was $0 \mu\text{M}$. Note that the amount of DAG produced by Oxo-M is a bit smaller, with VSP activation. This results from the clearance of “excess” PI(4)P by the 4-phosphatase as observed in A.

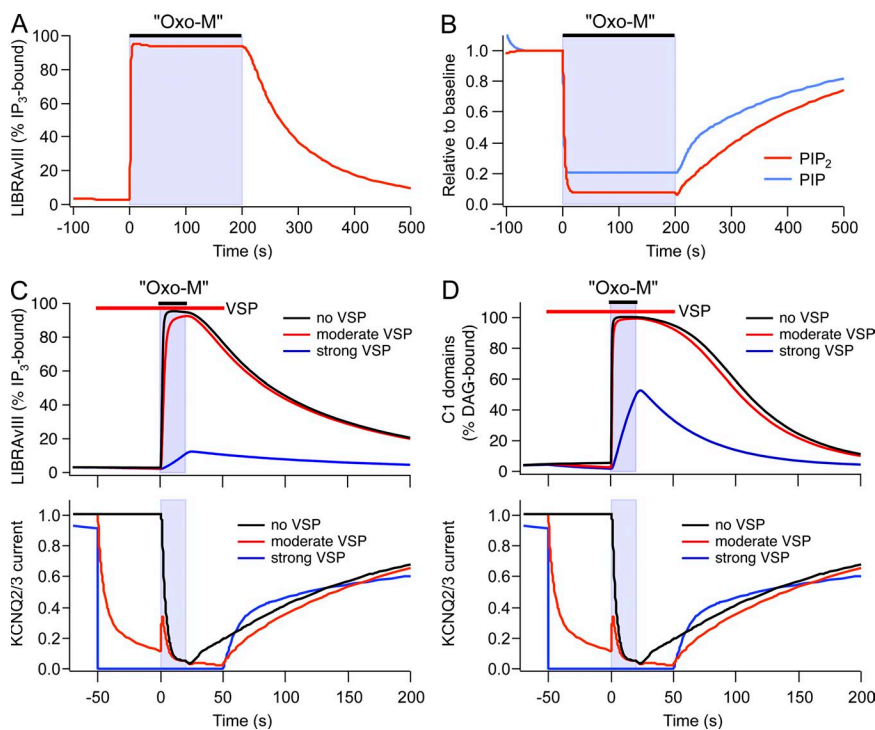


Figure S6. Trial model without PIP hydrolysis by PLC. A model was constructed without PIP hydrolysis by PLC. (A) Without IP_2 generation from PIP, the PI 4-kinase needs to be stimulated less to sustain the LIBRAvIII response during 200 s of Oxo-M. Thus, during agonist, k_{4K} was accelerated only to 0.0043 s^{-1} instead of 0.006 s^{-1} in the standard model (see Fig. 7 F in the main text). (B) Without PIP hydrolysis by PLC, the PI 5-kinase needs to be stimulated more to deplete PIP by 80% as observed biochemically (Horowitz et al. 2005. *J. Gen. Physiol.* 126:243–262). Thus, k_{5K} was accelerated to 0.82 s^{-1} instead of 0.6 s^{-1} in the standard model. (C and D) Computed time courses of LIBRAvIII saturation, C1 saturation, and KCNQ2/3 current in a simulation as in Fig. 4 (G and H) in the main text, except for the changes noted above. VSP_max was 0 for “no VSP,” 0.3 s^{-1} during “moderate” VSP activation, and 150 s^{-1} during “strong” VSP activation. Note that when the LIBRAvIII response is inhibited with “strong VSP,” the C1 response is as well. This contradicts our experimental findings (Fig. 4 in the main text). $[\text{LIBRAvIII}]$ was $6 \mu\text{M}$, and $[\text{C1}]$ was $0.5 \mu\text{M}$.